Results in Surfaces and Interfaces 18 (2025) 100437

Contents lists available at ScienceDirect

Results in Surfaces and Interfaces

journal homepage: www.elsevier.com/locate/rsurfi

Femtosecond laser polishing of pure copper surfaces with perpendicular incidence

Emmanuel Loubère [a], Nada Kraiem [a,c], Aofei Mao [c], Sébastien Preaud [a], Andrzej Kusiak [b], Amélie Veillère [a], Jean-François Silvain [a,c,**], Yong Feng Lu [c,*]

[a] Univ. Bordeaux, CNRS, Bordeaux INP, ICMCB, UMR 5026, Pessac, France
[b] Institute of Mechanics and Mechanical Engineering (I2M), UMR 5295, Talence, France
[c] Department of Electrical and Computer Engineering, University of Nebraska, Lincoln, NE, USA

ARTICLE INFO

Keywords:
Femtosecond laser
Laser polishing
Perpendicular incidence
Copper

ABSTRACT

Over the past few years, femtosecond (fs) laser processing has drawn a growing interest in a wide range of applications as it offers the possibility to process the surface morphologies of metals and semiconductors. In contrast to other polishing techniques, laser polishing offers a flexible and non-contact solution, thereby avoiding potential external contamination, while enabling a precise selection of processing areas. We investigated the influence of fs laser parameters on surface roughness of pure copper and ablation thickness, focusing on highlighting the importance of fluence and scanning overlap. With a two-step processing strategy, composed of coarse and fine polishing steps, surfaces with $Sa < 400$ nm were achieved, representing a 98% reduction from the high roughness of 15 μm on initial surfaces. This research demonstrated the possibility of directly polishing rough parts using a fs laser with a perpendicular incidence.

1. Introduction

Control of surface characteristics have been a field of great interest for many years due to their significant impact on material properties (Gravier et al., 2012; Toloei et al., 2013; Evgeny et al., 2016; Pegues et al., 2018; Leon and Aghion, 2017; Sanaei and Fatemi, 2020; Bayoumi and Abdellatif, 1995). Pegues et al. showed that the high surface roughness (Sa ≈10–25 μm) of additive-manufactured Ti–6Al–4V specimens was responsible for a low fatigue limit of approximately 110 MPa, in comparison to a 550–750 MPa range for wrought Ti–6Al–4V (Pegues et al., 2018). Toloei et al. showed on pure nickel sheets that *Sa* of the metal surface has a major influence on corrosion resistance. The lower the surface roughness is, the higher the corrosion resistance would be (Toloei et al., 2013). Although numerous parameters can be used to describe surface roughness, the profile (R_a) and surface (S_a) arithmetic average roughness heights are the most commonly used in literature. To get the lowest average surface roughness possible, mechanical, chemical, and thermal surface finishing solutions have been developed to treat both internal and external roughness (Lee et al., 2021). Each technique presents distinct advantages and limitations. Selection of appropriate techniques depends on specific applications.

Mechanical polishing is based on material removal through abrasion by a harder material. Submicron scale roughness can be achieved but it is time-consuming, not suitable for complex shapes with contamination from the abrasive tools (Tournier, 1982). Chemical polishing, which relies on chemical reactions to smooth surfaces, enables submicron-scale roughness on both external and internal surfaces of simples and complex structures. However, its applicability is constrained to a limited selection of materials and lacks precision, in addition to environmental and safety concerns (Jacquet; Tuck, 1975). To enhance removal rates, chemical and mechanical actions can be combined, known as chemical mechanical polishing, but this leads to a higher level of process complexity and necessitates specific equipment (Zhao and Lu, 2013; Lee et al., 2016; Das et al., 2020). Thermal polishing employs electron beams, continuous wave (CW), or short pulse duration (about 10^{-9} s) lasers to melt and reflow material surfaces. In contrast to mechanical and chemical methods, it is a flexible non-contact solution that permits the selection of the area to be processed, avoids external contamination, and is cost and time-efficient. Nevertheless, CW or short pulse laser polishing does have its drawbacks, as an important heat-affected zone

* Corresponding author.
** Corresponding author. Univ. Bordeaux, CNRS, Bordeaux INP, ICMCB, UMR 5026, Pessac, France.
E-mail addresses: jean-francois.silvain@icmcb.cnrs.fr (J.-F. Silvain), ylu2@unl.edu (Y.F. Lu).

https://doi.org/10.1016/j.rsurfi.2025.100437
Received 27 December 2024; Received in revised form 20 January 2025; Accepted 23 January 2025
Available online 31 January 2025

(few to several tens of μm, depending on laser parameters and materials), potential composition and microstructural changes, and dependence on initial surface roughness (Sedao et al., 2022; Audouard, 2023; Krishnan and Fang, 2019).

Over the last decades, ultrashort pulse laser (10^{-15}-10^{-18} s) machining has drawn growing interest in various fields due to their ability to process all material types, with high resolution and little or no thermal effects to surrounding areas, in contrast to longer pulse duration lasers (Le Harzic et al., 2002; Rizvi et al., 2001; Chichkov et al., 1996). This ability comes from the extremely intense peak power reached by the ultrashort pulses, which makes possible net ablation, by multi-photon ionization and matter ejection (Le Harzic et al., 2002; Valette; Liu et al., 1997; Von Der Linde et al., 1997). Few studies have explored metal polishing using a femtosecond (fs) laser. Among them, Yang et al. (Fan et al., 2019) and Schnell et al. (2020) studied the influence of laser fluence and overlapping rate of the laser beam on Ti–6Al–4V with low initial roughness of approximately 0.065 μm (Fan et al., 2019). They showed that a lower fluence is more beneficial to reduce surface roughness and the size of surface nanoparticles increases with the increase in the pulse overlapping. Li et al. (2023) studied the fs laser polishing of stainless steel additively manufactured. They showed that parallel-incidence permits surface roughness reduction from $Sa >$ 20 μm to $Sa = 0.2$ μm by successive layer ablation, whereas $Sa < 3.2$ μm cannot be achieved with the perpendicular incidence where a simultaneous ablation occurs.

With the energy transition and electrification applications, copper (Cu) has shown a significantly increasing demand for its good thermal and electrical properties. As this trend is expected to grow further, mastering Cu post-processing is essential. Due to its unique flexibility, laser polishing has promising potential. However, Cu is a challenging material to laser process due to its low absorptivity (A) to the most common lasers with infrared wavelength ($A = 5\%$ for $\lambda = 1064$ nm (Domine et al., 2023)). To overcome this low absorptivity, potential solutions are the use of a high incident laser power or a laser wavelength for which Cu has a better absorptivity (e.g., green laser $\lambda = 515$ nm, $A =$ 44 % (Domine et al., 2023)). Grub et al. (2022) used a CW laser with a visible green wavelength of 515 nm and a maximum output power of 1000 W on Cu parts produced by laser powder bed fusion. They reduced the average surface roughness from $Sa = 21.6$ to 3.2 μm. The laser wavelength has little or no influence due to the high peak power delivered by the fs laser pulses. The absorption mainly depends on the amount of incident energy, making fs laser suitable for processing copper (Audouard, 2023). Chen et al. (2022) studied the fs laser processing of Cu surfaces with initial nanoscale *Sa* and demonstrated the possibility of achieving a surface with $Sa = 0.056$ μm by employing a crossover strategy and varying pulse overlap rates. Zemaitis et al. (Žemaitis et al., 2021) conducted an in-depth experimental study on the high ultrafast laser ablation efficiency of copper, exploring single-pulse, MHz, GHz, and biburst regimes.

However, fs laser polishing of pure Cu has not yet been extensively studied and requires further investigation. While nanometric-scale roughness has been achieved in previous studies, these outcomes are generally limited to surfaces that initially exhibit nanometric-scale roughness before treatment. To the best of our knowledge, the reduction of high initial surface roughness to a submicron level through fs laser polishing of Cu has not yet been investigated.

This study aimed to demonstrate the effectiveness of fs laser polishing on pure Cu with a high initial surface roughness Sa ≈15 μm. We investigated the influence of laser parameters [pulse energy, scanning speed, hatch distance (h), and scanning time (ST)] on surface roughness and ablation thickness, highlighting the importance of carefully choosing pulse energy and overlap to achieve a final surface roughness below 0.4 μm with an initial surface roughness of 15 μm. This research showed the possibility of easily and directly polishing parts using a fs laser with perpendicular incidence and could be extended to the polishing of specific areas on complex parts additively manufactured.

2. Materials and methods

2.1. Equipment

The laser polishing was conducted in ambient atmosphere using a Tangor laser system which works at a wavelength of 1030 nm and delivers pulses of 400 fs (Amplitude Laser, Inc.). The p-polarized laser beam was scanned by a galvanometer scanner (SCANLAB GmbH) and focused to a 15 μm spot diameter by an F-theta lens with a focal length of 70 mm. Before and after each laser processing, surface roughness was measured in an area of 1.7×1.7 mm^2 using an × 20 objective lens of the optical surface profiler Zygo NewView 8000 3D. Line profile measurement, and their Amplitude Spectrum Density (ASD), have been performed using the Zygo software. The ablated thickness has been measured using the optical surface profiler. Detailed surface characterization has been performed using a Hitachi S4700 field-emission scanning electron microscope (FE-SEM).

2.2. Specimen

Laser polishing experiments were performed on a pure Cu sample fabricated by powder metallurgy method [uniaxial hot pressing (50 MPa, 650 °C, 30 min, primary vacuum)] and sandblasted using an Arena Blast equipment. The initial average surface roughness was in the range of 15 μm and was composed of randomly spaced peaks and valleys, with a maximum peak-to-valley roughness up to 150 μm.

2.3. Method

The study aimed to establish a link between the numerous fs laser parameters and the final surface roughness of pure copper. All experiments were performed at a focal distance with a constant spot diameter of 15 μm and with an incidence perpendicular to the sample surface.

Ancona et al. (2009) showed that repetition rates between 100 and 975 kHz for 800 fs pulses at 1030 nm have almost no impact on the ablation efficiency of pure copper, what Sedao et al. (2019) confirmed later for repetition rates between 31 and 500 kHz for 350 fs pulses with a constant overlap of 91%. Therefore, we decided to fix the pulse frequency to f = 330 kHz to reduce processing time and ensure a similar time interval of 3 μs between successive pulses in each experiment. Squares of 2.3×2.3 mm^2 were processed with a 90° rotation between each scanning to avoid preferential orientation of the final surface (Appendix 1). Laser parameters studied are hatch distance [2–15 μm], pulse energy [7.5–30 μJ], scanning speed [1–5 m/s], and scanning time [up to 2400]. For a Gaussian laser beam, the energy distribution is not uniform across the spot diameter. The energy reaches its maximum at the center and decreases radially. Ablation processes are governed by the local energy density surpassing the ablation threshold, making the maximum fluence (F_{max}) the key parameter for determining the onset of material removal. For a Gaussian laser beam, F_{max} can be expressed as:

$$F_{max} = \frac{2\,PE}{\pi\, w^2} \tag{1}$$

with PE = pulse energy (J), w = radius of the laser spot (cm).

3. Results and discussions

3.1. Femtosecond laser top surface polishing optimization

3.1.1. Influence of line overlap

The Line Overlap (O_L) represents the overlap between two laterally adjacent laser tracks and depends on hatch distance and beam spot diameter (Eq. (2)). In our study, beam diameter is considered a constant (15 μm) as all experiments were performed at the focal distance. Different line overlaps (O_L) were obtained by changing the value of

hatch distance at a fixed pulse energy (PE) of 15 µJ. $O_L = 0$ % means there is no overlap between two successive laser tracks, whereas $O_L = 87$ % means the laser track N+1 is performed on 87 % of the previous laser track N width (Fig. 1a).

$$O_L = \left(1 - \frac{h}{D}\right) \times 100 \tag{2}$$

with h the hatch distance (µm) and D the beam spot diameter (µm).

At a pulse energy tested, higher line overlap leads to more thickness ablation (Fig. 1b). This phenomenon can be explained by the fact that for higher line overlap, more laser tracks and pulses are applied in the same surface unit. Surface roughness does not evolve linearly with the line overlap increasing. For O_L from 0% to 67%, final surface roughness tends to decrease with the increase in O_L, with the lower average surface roughness Sa = 2.9 µm reached at $O_L = 67$ % (Fig. 1b).

Increasing the line overlap enables processing the entire surface of the sample, without unprocessed space between laser tracks. Moreover, it enables a higher ablation rate and then increases the chances of flattening the surface by the removal of peaks. However, the increase of O_L beyond 67 % does not lead to a lower Sa. The choice of $O_L = 67$ %, which corresponds to a hatch distance of 5 µm, is made for the following experiments.

3.1.2. *Influence of pulse energy and overlap*

Pulse Overlap describes the overlap between two consecutive pulses. This indicator establishes a relationship between beam diameter, laser scanning speed, pulse frequency, and duration (Equation (3)). The pulse frequency is set to 330 kHz to reduce processing time and ensure a constant interval between successive pulses in each experiment. As the laser beam diameter and pulse duration were kept constant in our experiments, the pulse overlap is determined only by laser scanning speed. With all parameters being constants, an increase in the scanning speed will spatially separate pulses and then decrease pulse numbers applied on the surface. For pulse energies of 7.5, 10, 15, 20, and 30 µJ, corresponding to $F_{max} = 8.5$, 11.3, 17, 22.6, and 34 J/cm^2, scanning speed (v) was varied to obtain pulse overlaps of $O_P = -1$, 29, 50, 68, and 80 % (Fig. 2).

$$O_P = \left(1 - \frac{\frac{v}{f}}{D + v^*\tau}\right) \times 100 \tag{3}$$

with v the scanning speed (m/s), f the frequency (Hz), D the beam spot diameter (µm), and τ the pulse duration (s).

Concerning the evolution of surface roughness (Fig. 2a), in a general tendency, for F_{max} = 8.5–17 J/cm^2, increasing both pulse energy and overlap enables a better reduction of the surface roughness. Beyond 17 J/cm^2, increasing the pulse overlap up to 67% has no noticeable effect, or even a worse outcome if increased to 80%. At a high pulse overlap (80%), increasing F_{max} to 34 J/cm^2 has a negative effect on the surface roughness, with a final roughness of 8.3 µm. Sedao et al. (2019) noticed the same tendency with an increase in the surface roughness from 20 to 500 nm with increasing the fluence from 0.6 to 18 J/cm^2.

The ablation threshold of Cu ($F_{th\ Cu}$) is experimentally calculated by measuring the width and depth of the ablation profile for different fluences (Appendix 2). $F_{th\ Cu}$ is exceeded for all pulse energies tested. Part of the pulse energies beyond the ablation threshold were used for

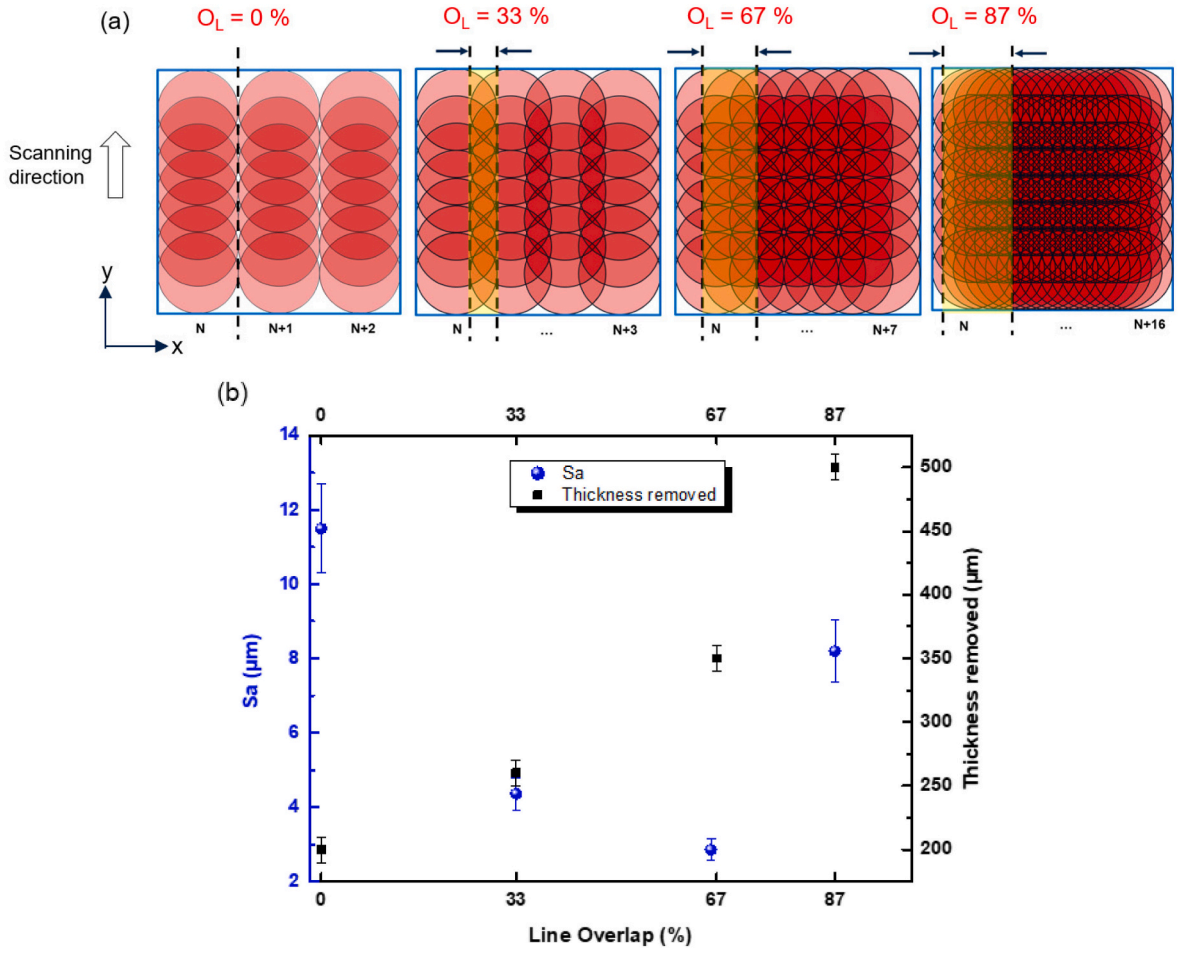

Fig. 1. (a) Schematic of laser tracks for different OL (b) Influence of OL on average roughness and thickness removed. (ST = 600; OL = 67 %).

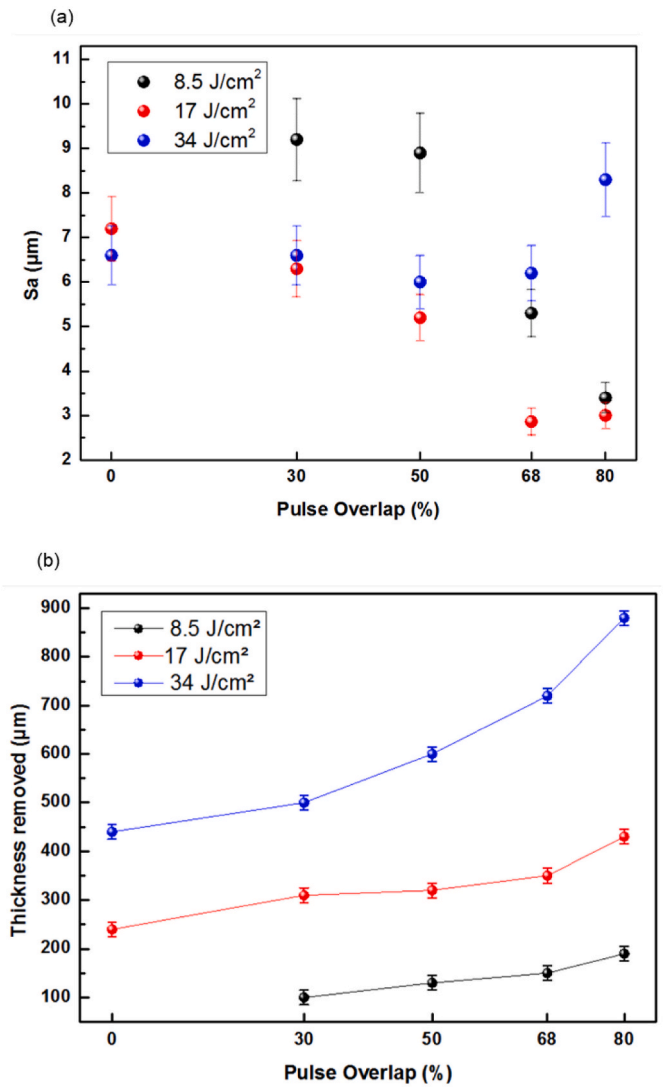

Fig. 2. Influence of pulse energy and overlap on (a) average roughness and (b) thickness removed.

material ablation, but the rest is thermally dissipated and can affect the processing quality. Thus, more energy is dissipated in the bulk material when pulse energy and fluence are increased. Even if fs laser processing is considered as non-thermal, plenty of studies reported heat accumulation and particle shielding effects affecting the ablation quality with high repetition rates (at a few kHz) (Eaton et al., 2005; Schille et al., 2010, 2012; Schnell et al., 2021). These phenomena are material dependent. For high repetition rates, the possibility that pulse energy is not dissipated when the following pulse is applied, causing a temperature rise and modifies the phenomenon of laser-matter interactions.

Nevertheless, studies on Cu showed that heat accumulation in fs laser processing at a high repetition rates is negligible due to the high thermal conductivity of copper (Ancona et al., 2009; Sedao et al., 2019; Schille et al., 2012). Thermal electron-lattice equilibrium is typically reached within approximately 10 ps, with subsequent cooling occurring around 1 ns. These timeframes are notably shorter than the interval of 3 µs (equivalent to a frequency of 330 kHz) between two successive 400-fs -long pulses. Heat accumulation in the case of Cu would occur with higher repetition rates, in the range of GHz (i.e., 1 ns between successive pulses) (Valette; Le Harzic et al., 2005; Audouard and Mottay, 2023). Although the heat should be dissipated before the impact of the next pulse, it is more beneficial to avoid the application of excessively energetic pulses. The lowest surface roughness S_a = 2.9 µm is achieved with 68% overlapped 15 µJ pulses, corresponding to 17 J/cm^2.

Concerning the ablation thickness, at equal F_{max}, material ablation is increased as pulse overlap increases because more pulses are applied to the same area, as discussed for line overlap in section 3.1.1. At equal pulse overlap, material ablation is increased as F_{max} increases due to the deeper ablation following the well-known logarithmic dependence of the ablation depth on the laser fluence (Preuss et al.; Chicbkov et al.). Ablation rates are enhanced through higher F_{max} and increased overlap.

Optimal conditions for reducing surface roughness while minimizing material ablation have been found by applying a F_{max} of 17 J/cm^2, an overlap of 68%, and conducting 600 scanning time. Following these parameters, defined as coarse polishing parameters, a remarkable 79% reduction in surface roughness (from an initial *Sa* of 14 µm) was observed with an ablation of 350 µm thickness.

3.1.3. *Influence of scanning times*

The lowest surface roughness of *Sa* ≈ 3 µm obtained with experiments presented in (Fig. 2a), is also the limit attained by Li et al. (2023) on top-surface fs laser polishing of stainless steels, and by Grub et al. (2022) on polishing copper with a green laser. To obtain a lower surface roughness, we studied the impact of scanning times with the coarse polishing parameters described previously in 3.1.2. By increasing them to 1200 and 1800, surface roughness was respectively reduced to *Sa* = 1.3 and 1 µm (Fig. 3). However, the impact of scanning times beyond 1200 appears to diminish, as there is a slight reduction in surface roughness between 1200 and 1800 scanning times, reaching a plateau at about 1 µm.

3.1.4. *Multistep polishing*

To address surface roughness exceeding 1 µm, we implemented a two-step polishing strategy by adjusting the applied fluences to enable ablation in two distinct regimes. When the fluence significantly exceeds the ablation threshold (F_{th}), strong ablation dominates, effectively removing large surface asperities. Conversely, when the fluence is slightly above F_{th}, gentle ablation occurs, allowing for finer smoothing of the surface. This approach ensures the efficient removal of rough features while achieving a finely polished surface.

The polishing process begins with a coarse polishing step, where $F_{max,\ coarse}$ is set significantly higher than $F_{th,\ Cu}$, enabling strong ablation to reduce surface roughness from 10–15 µm to 2–4 µm. This is followed by a fine polishing step, where $F_{max,\ fine}$ is adjusted to be slightly above $F_{th,\ Cu}$, allowing gentle ablation to achieve a final surface roughness below Sa≈0.4 µm. By lowering the pulse energy and fluence in the fine polishing step, the ablation quality is enhanced, resulting in an improved final surface finish. The choice of increasing pulse overlap for the finishing step is based on the results shown in Fig. 2a, where roughness is better reduced with O_y = 80 % than 68% for F_{max} = 8.5 J/cm^2. Recently, research has been conducted on fs laser metal processing employing a multistep strategy and adjusting pulse energy accordingly. Li et al. (2023) and Leggio et al. (2023) showed that a decreased gradient fluence sequence leads to a lower surface roughness than a uniform or increasing gradient sequence. The concept of a multistep strategy can be likened to mechanical polishing, wherein the grain size of the polishing tools is progressively refined throughout the process.

3.2. *Surface characterization*

Line profiles (Fig. 4) provide surface characteristics along a specific direction and give a complementary representation to the three-dimensional analysis (Fig. 3). The line profile measurements clearly show the roughness reduction of the high peaks and valleys in the range of tens of micrometers from the initial surfaces to the submicron scale roughness after the coarse and fine polishing steps. Amplitude Spectral Density (ASD), which illustrates how the amplitude of the line profile signal is distributed among different spatial frequencies, was computed for each line profile using the Zygo software. The ASD of the data

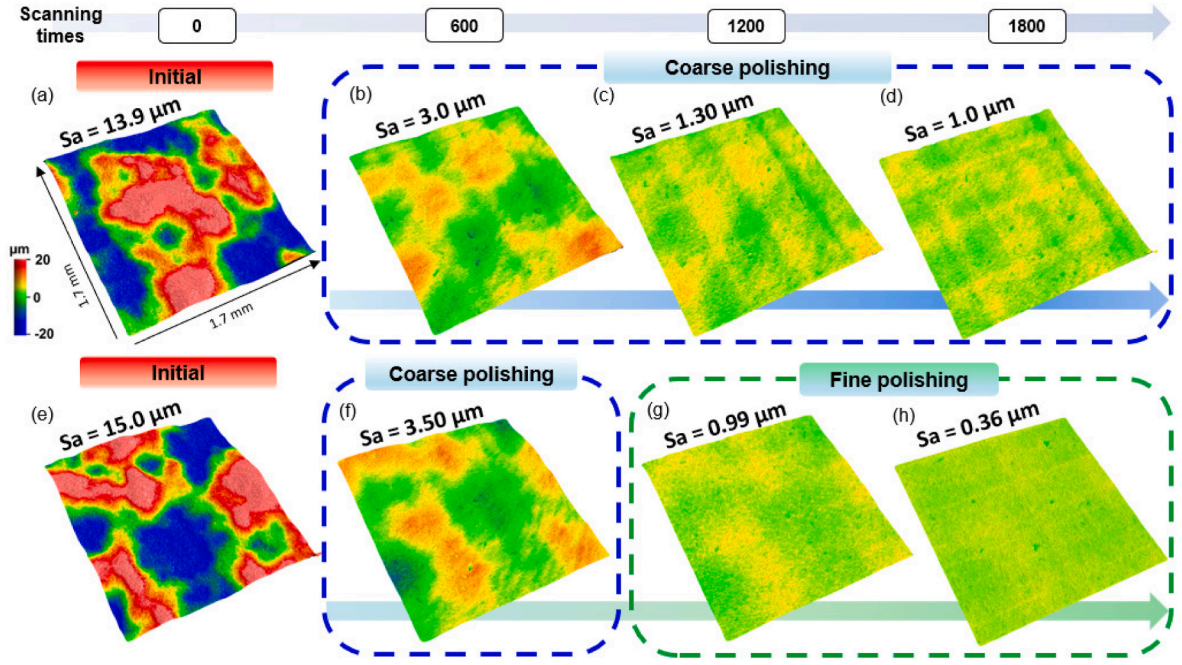

Fig. 3. Representative optical profiler images of (a,e) initial (b-d,f) coarse and (g,h) fine polished surfaces.

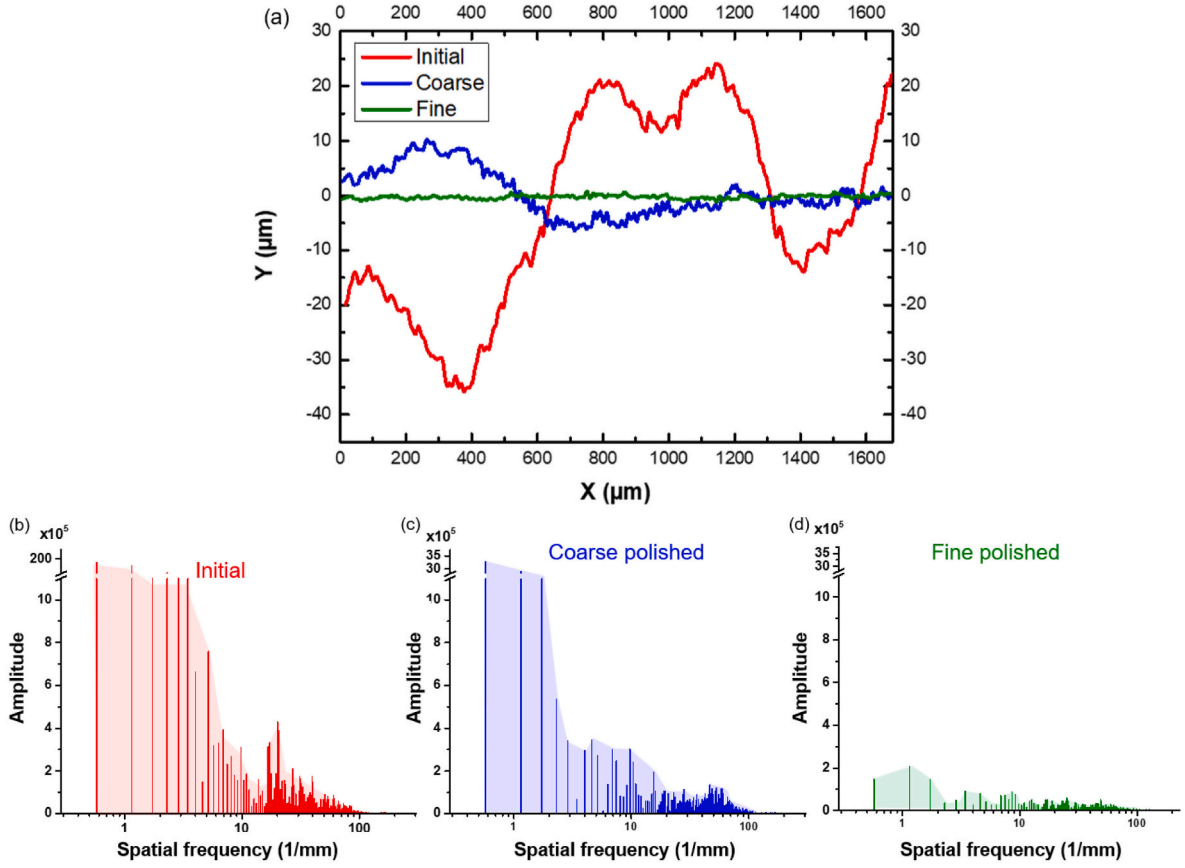

Fig. 4. Characterization of initial, coarse, and fine polished surface roughness: (a) representative line profiles and (b–d) their amplitude associated spectra.

obtained from the line profile analysis performed on the initial surface mainly consists of numerous peaks with high amplitude and low frequency, as well as peaks with low amplitude and high frequency, indicating the presence of high and spaced peaks and valleys on which there are smaller peaks close to each other. ASD corresponding to the line profiles on the surfaces polished with coarse polishing parameters exhibits amplitude and quantity-reduced peaks compared to the ASD of the initial surfaces, illustrating a roughness reduction. The presence of a few

high-amplitude and low-frequency peaks and low-amplitude and high-frequency peaks indicates a two-scale roughness, with a smaller roughness on more periodically spaced peaks. In contrast to the former two, the ASD of the fine-polished surfaces mainly exhibits low amplitude and high-frequency peaks, depicting small and low-spaced peaks and valleys.

Micrographs from Scanning Electron Microscopy (Fig. 5) illustrate and complement these numerical roughness characterizations. Randomly distributed peaks and valleys are observable on the initial surfaces (Fig. 5a and 5d) whereas Laser-Induced Periodic Surface Structures (LIPSS) can be seen after laser polishing (Fig. 5e and 5f). LIPSS or ripples are a well-known and studied phenomenon that results from laser/matter interactions. Their periodicity and size vary from a few nanometers to micrometers, depending on the laser parameters applied, whereas their orientation and shape depend on the laser polarization (Gräf and Müller, 2015; Nakajima et al., 2022; Gnilitskyi et al., 2023; Bizi-bandoki et al., 2013; Reif et al., 2009). Following the coarse polishing step, a two-scale surface morphology appears with linear features aligned with the last scanning direction and spaced a few micrometers apart with an undefined periodicity, on which stand ripples with periodicity within the range of laser wavelength. Since the repetition rate and scanning speed utilized should not cause any thermal impact and grooves are typically aligned parallel to the laser polarization direction (Gnilitskyi et al., 2023; Bizi-bandoki et al., 2013), the linear features seem to arise from laser tracks and interferences triggered by the initial high surface roughness of the sample. After the fine polishing step, the surface is composed of ripples spaced with a periodicity close to the laser wavelength, also called low-spatial-frequency LIPSS (LSFL) (Bonse et al., 2012).

3.2.1. Comparison with literature

Fig. 6 illustrates a comparative analysis between our findings and results of previous research focusing on surface polishing with perpendicular incidence on samples with high initial surface roughness. Other studies typically attain a roughness limit around Sa = 2.5–3 µm following laser processing using CW, ns, or fs lasers. A submicron surface roughness Sa <400 nm was reached in our study, highlighting the importance of carefully choosing laser parameters and scanning strategy, especially employing a multistep strategy. The comparison with the work of Grub et al. (2022), who obtained a final arithmetic roughness of 3.2 µm, reveals the advantage of using a fs laser over CW one to laser polish copper. Ultrashort pulse laser polishing has no wavelength dependence and overcomes the low laser absorption of copper in the infrared domain. This characteristic enables achieving a high polishing quality via ablation, in comparison to polishing via melting with CW lasers.

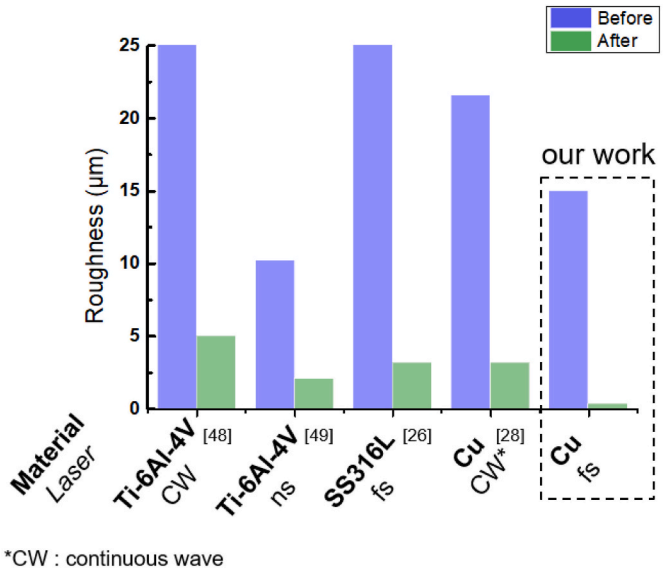

Fig. 6. Literature review of studies on perpendicular-incidence laser polishing (Li et al., 2023; Grub et al., 2022; Genna and Rubino, 2019; Liang et al., 2020).

4. Conclusion

We studied using a fs laser with a perpendicular incidence to polish rough Cu surfaces. We studied the impact of line and pulse overlap, pulse energy, and scanning time on surface roughness and ablation thickness. We showed that laser parameters must be chosen carefully to obtain a sub-micrometer average surface roughness. By applying a two-step

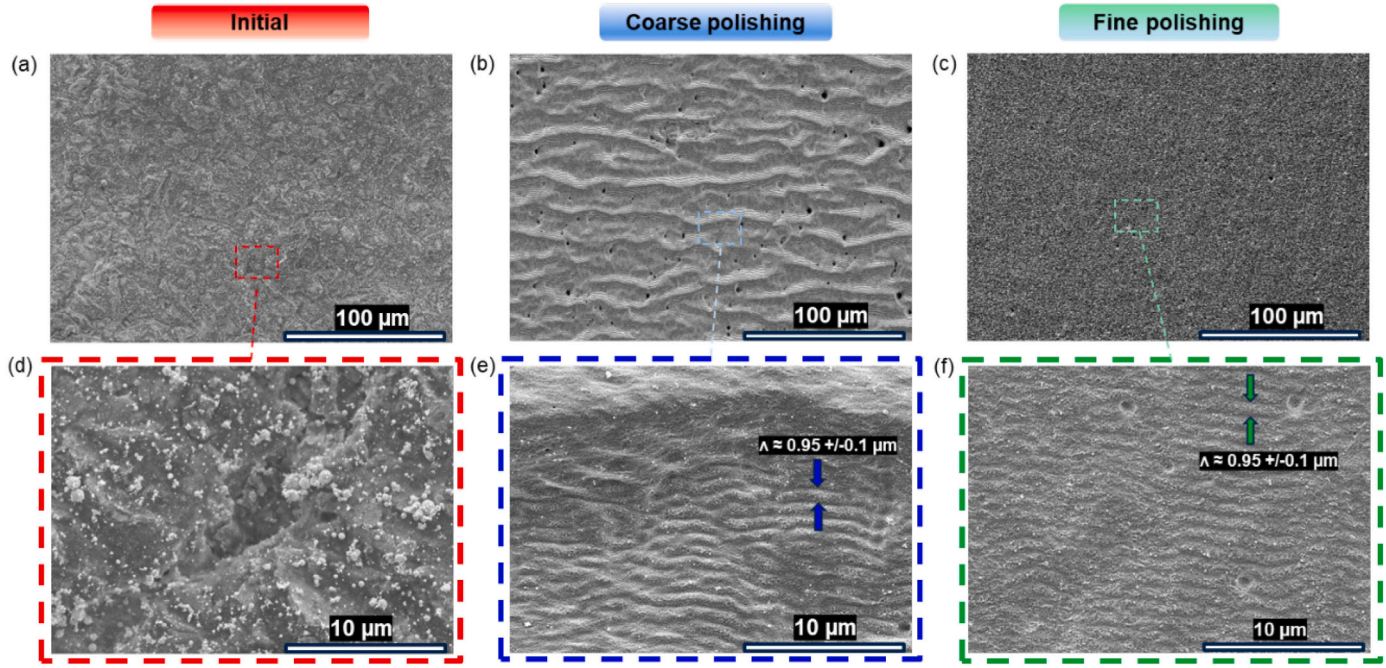

Fig. 5. SEM micrographs of a,d) initial, (b,e) coarse, and (c,f) fine polished surfaces.

strategy, composed of coarse and fine polishing steps, surfaces with $Sa <$ 400 nm were achieved representing a 98% reduction from the high initial surface roughness of 15 µm. This study shows that fs laser polishing can be a post-manufacturing solution for Cu parts with high initial surface roughness ($Sa = 12$–15 µm). The method to properly define laser polishing parameters can be applied to other types of materials with more sophisticated structures. The use of a top-hat fs laser or the combination with a ns laser to slightly remelt the LIPSS are potential perspectives to achieve nanoscale surface roughness.

CRediT authorship contribution statement

Emmanuel Loubère: Writing – original draft, Validation, Methodology, Investigation, Formal analysis, Data curation, Conceptualization. **Nada Kraiem:** Methodology, Investigation. **Aofei Mao:** Methodology, Investigation. **Sébastien Preaud:** Methodology, Investigation. **Andrzej Kusiak:** Methodology, Investigation. **Amélie Veillère:** Validation, Supervision, Resources, Project administration, Investigation, Funding acquisition, Formal analysis, Conceptualization. **Jean-François Silvain:** Writing – review & editing, Validation, Resources, Project administration, Investigation, Funding acquisition, Formal analysis, Conceptualization. **Yong Feng Lu:** Writing – review & editing, Supervision, Resources, Project administration, Methodology, Investigation, Funding acquisition, Formal analysis, Conceptualization.

Declaration of competing interest

The authors declare that they have no known competing financial interests or personal relationships that could have appeared to influence the work reported in this paper.

Acknowledgments

This study was carried out in the Laser Assisted Nano-Engineering Lab (LANE) at the University of Nebraska-Lincoln and supported by the Agence Nationale de la Recherche (ANR) française (Project 3DCOMPOSITE, ANR-21-CE08-0015) and theFulbright program PS00358784.

Appendix

Appendix 1Scanning strategy: 90° rotation between each scanning time

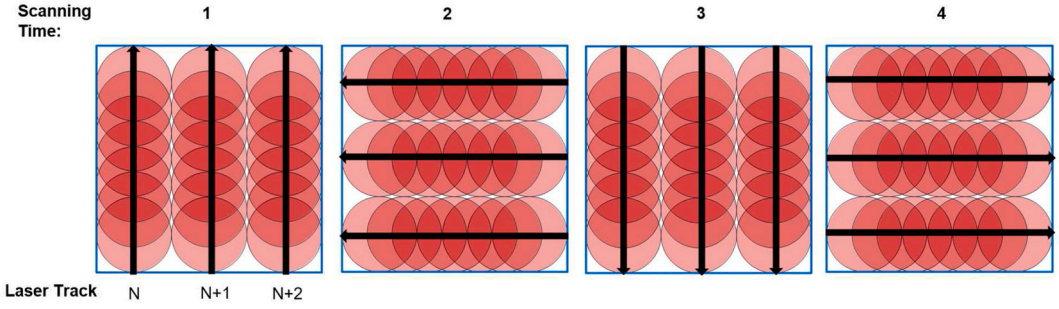

Appendix 2. Calculation of Cu ablation threshold

$$F_{th} = F_0 e^{-\left(\frac{w_{abl}}{2w_0}\right)^2}$$

F_{th} = Threshold fluence; F_0 = Peak fluence; W_{abl} = ablation width; W_0 = Beam waist.

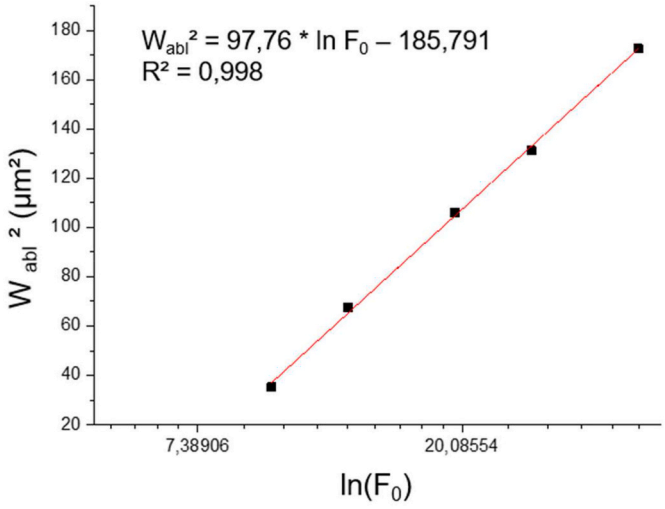

Data availability

Data will be made available on request.

References

Ancona, A., Döring, S., Jauregui, C., Röser, F., Limpert, J., Nolte, S., et al., 2009. Femtosecond and picosecond laser drilling of metals at high repetition rates and average powers. Opt. Lett. 34, 3304. https://doi.org/10.1364/OL.34.003304.

Audouard, É., 2023. Procédés laser femtoseconde - Applications industrielles des impulsions ultrabrèves. Optique Photonique. https://doi.org/10.51257/a-v2-e6455.

Audouard, E., Mottay, E., 2023. High efficiency GHz laser processing with long bursts. Int. J. Extrem. Manuf. 5, 015003. https://doi.org/10.1088/2631-7990/aca79f.

Bayoumi, M.R., Abdellatif, A.K., 1995. Effect of surface finish on fatigue strength. Eng. Fract. Mech. 51, 861–870. https://doi.org/10.1016/0013-7944(94)00297-U.

Bizi-bandoki, P., Valette, S., Audouard, E., Benayoun, S., 2013. Effect of stationary femtosecond laser irradiation on substructures' formation on a mold stainless steel surface. Appl. Surf. Sci. 270, 197–204. https://doi.org/10.1016/j.apsusc.2012.12.168.

Bonse, J., Krüger, J., Höhm, S., Rosenfeld, A., 2012. Femtosecond laser-induced periodic surface structures. J. Laser Appl. 24, 042006. https://doi.org/10.2351/1.4712658.

Chen, C., Kuong Ng, C., Zhang, F., Xiong, X., Ju, B.-F., Zhang, Y., et al., 2022. Towards obtaining high-quality surfaces with nanometric finish by femtosecond laser ablation: a case study on coppers. Opt Laser. Technol. 155, 108382. https://doi.org/10.1016/j.optlastec.2022.108382.

Chicbkov BN, Momma C, Nolte S. Femtosecond, Picosecond and Nanosecond Laser Ablation of Solids n.d.

Chichkov, B.N., Momma, C., Nolte, S., 1996. Femtosecond, picosecond and nanosecond laser ablation of solids. Phys A 63, 109–115. https://doi.org/10.1007/BF01567637.

Das, S., Kibria, G., Doloi, B., Bhattacharyya, B. (Eds.), 2020. Advances in Abrasive Based Machining and Finishing Processes. Springer International Publishing, Cham. https://doi.org/10.1007/978-3-030-43312-3.

Domine, A., Verdy, C., Penaud, C., Vitu, L., Feneniche, N., Dembinski, L., 2023. Selective laser melting (SLM) of pure copper using 515-nm green laser: from single track analysis to mechanical and electrical characterization. Int. J. Adv. Manuf. Technol. https://doi.org/10.1007/s00170-023-12338-5.

Eaton, S.M., Zhang, H., Herman, P.R., Yoshino, F., Shah, L., Bovatsek, J., et al., 2005. Heat accumulation effects in femtosecond laser-written waveguides with variable repetition rate. Opt Express 13, 4708. https://doi.org/10.1364/OPEX.13.004708.

Evgeny, B., Hughes, T., Eskin, D., 2016. Effect of surface roughness on corrosion behaviour of low carbon steel in inhibited 4 M hydrochloric acid under laminar and turbulent flow conditions. Corrosion Sci. 103, 196–205. https://doi.org/10.1016/j.corsci.2015.11.019.

Fan, W., Yang, Y., Lou, R., Chen, X., Bai, J., Cao, W., et al., 2019. Influence of energy fluence and overlapping rate of femtosecond laser on surface roughness of Ti-6Al-4V. Opt. Eng. 58, 1. https://doi.org/10.1117/1.OE.58.10.106107.

Genna, S., Rubino, G., 2019. Laser finishing of Ti6Al4V additive manufactured parts by electron beam melting. Appl. Sci. 10, 183. https://doi.org/10.3390/app10010183.

Gnilitskyi, I., Bellucci, S., Marrani, A.G., Shepida, M., Mazur, A., Zozulya, G., et al., 2023. Femtosecond laser-induced nano- and microstructuring of Cu electrodes for CO2 electroreduction in acetonitrile medium. Sci. Rep. 13, 8837. https://doi.org/10.1038/s41598-023-35869-z.

Gräf, S., Müller, F.A., 2015. Polarisation-dependent generation of fs-laser induced periodic surface structures. Appl. Surf. Sci. 331, 150–155. https://doi.org/10.1016/j.apsusc.2015.01.056.

Gravier, J., Vignal, V., Bissey-Breton, S., 2012. Influence of residual stress, surface roughness and crystallographic texture induced by machining on the corrosion behaviour of copper in salt-fog atmosphere. Corrosion Sci. 61, 162–170. https://doi.org/10.1016/j.corsci.2012.04.032.

Grub, P., Hofele, M., Schanz, J., Kolb, D., Riegel, H., 2022. Laser polishing of additive manufactured L-PBF copper parts with visible laser wavelength of 515 nm – challenges due to high surface roughness. Procedia CIRP 111, 684–688. https://doi.org/10.1016/j.procir.2022.08.009.

Jacquet PA. Electrolytic and chemical polishing n.d.

Krishnan, A., Fang, F., 2019. Review on mechanism and process of surface polishing using lasers. Front. Mech. Eng. 14, 299–319. https://doi.org/10.1007/s11465-019-0535-0.

Le Harzic, R., Huot, N., Audouard, E., Jonin, C., Laporte, P., Valette, S., et al., 2002. Comparison of heat-affected zones due to nanosecond and femtosecond laser pulses using transmission electronic microscopy. Appl. Phys. Lett. 80, 3886–3888. https://doi.org/10.1063/1.1481195.

Le Harzic, R., Breitling, D., Weikert, M., Sommer, S., Föhl, C., Valette, S., et al., 2005. Pulse width and energy influence on laser micromachining of metals in a range of 100fs to 5ps. Appl. Surf. Sci. 249, 322–331. https://doi.org/10.1016/j.apsusc.2004.12.027.

Lee, H., Lee, D., Jeong, H., 2016. Mechanical aspects of the chemical mechanical polishing process: a review. Int. J. Precis. Eng. Manuf. 17, 525–536. https://doi.org/10.1007/s12541-016-0066-0.

Lee, J.-Y., Nagalingam, A.P., Yeo, S.H., 2021. A review on the state-of-the-art of surface finishing processes and related ISO/ASTM standards for metal additive manufactured components. Virtual Phys. Prototyp. 16, 68–96. https://doi.org/10.1080/17452759.2020.1830346.

Leggio, L., Di Maio, Y., Pascale-Hamri, A., Egaud, G., Reynaud, S., Sedao, X., et al., 2023. Ultrafast laser patterning of metals commonly used in medical industry: surface roughness control with energy gradient pulse sequences. Micromachines 14, 251. https://doi.org/10.3390/mi14020251.

Leon, A., Aghion, E., 2017. Effect of surface roughness on corrosion fatigue performance of AlSi10Mg alloy produced by Selective Laser Melting (SLM). Mater. Char. 131, 188–194. https://doi.org/10.1016/j.matchar.2017.06.029.

Li, N., Fan, P., Zhu, Q., Cui, B., Silvain, J.-F., Lu, Y.F., 2023. Femtosecond laser polishing of additively manufactured parts at grazing incidence. Appl. Surf. Sci. 612, 155833. https://doi.org/10.1016/j.apsusc.2022.155833.

Liang, C., Hu, Y., Liu, N., Zou, X., Wang, H., Zhang, X., et al., 2020. Laser polishing of Ti6Al4V fabricated by selective laser melting. Metals 10, 191. https://doi.org/10.3390/met10020191.

Liu, X., Du, D., Mourou, G., 1997. Laser ablation and micromachining with ultrashort laser pulses. IEEE J. Quant. Electron. 33, 1706–1716. https://doi.org/10.1109/3.631270.

Nakajima, A., Omiya, M., Yan, J., 2022. Generation of micro/nano hybrid surface structures on copper by femtosecond pulsed laser irradiation. Nanomanuf. Metrol. 5, 274–282. https://doi.org/10.1007/s41871-022-00135-9.

Pegues, J., Roach, M., Scott Williamson, R., Shamsaei, N., 2018. Surface roughness effects on the fatigue strength of additively manufactured Ti-6Al-4V. Int. J. Fatig. 116, 543–552. https://doi.org/10.1016/j.ijfatigue.2018.07.013.

Preuss S, Demchuk A, Stuke M. Sub-picosecond UV Laser Ablation of Metals n.d.

Reif, J., Costache, F., Varlamova, O., Jia, G., Ratzke, M., 2009. Self-organized regular surface patterning by pulsed laser ablation. Phys. Status Solidi (c) 6, 681–686. https://doi.org/10.1002/pssc.200880719.

Rizvi, N.H., Karnakis, D., Gower, M.C., 2001. Micromachining of Industrial Materials with Ultrafast Lasers. International Congress on Applications of Lasers & Electro-Optics. Laser Institute of America, Jacksonville, Florida, USA, pp. 1511–1520. https://doi.org/10.2351/1.5059821.

Sanaei, N., Fatemi, A., 2020. Analysis of the effect of surface roughness on fatigue performance of powder bed fusion additive manufactured metals. Theor. Appl. Fract. Mech. 108, 102638. https://doi.org/10.1016/j.tafmec.2020.102638.

Schille, J., Ebert, R., Loeschner, U., Scully, P., Goddard, N., Exner, H., 2010. In: Heisterkamp, A., Neev, J., Nolte, S., Trebino, R.P. (Eds.), High Repetition Rate Femtosecond Laser Processing of Metals, 758915. https://doi.org/10.1117/12.842600. San Francisco, California, USA.

Schille, J., Schneider, L., Hartwig, L., Loeschner, U., Ebert, R., Scully, P., et al., 2012. Characterisation of Interaction Phenomena in High Repetition Rate Femtosecond Laser Ablation of Metals. International Congress on Applications of Lasers & Electro-Optics. Laser Institute of America, Anaheim, California, USA, pp. 949–958. https://doi.org/10.2351/1.5062569.

Schnell, G., Duenow, U., Seitz, H., 2020. Effect of laser pulse overlap and scanning line overlap on femtosecond laser-structured Ti6Al4V surfaces. Materials 13, 969. https://doi.org/10.3390/ma13040969.

Schnell, G., Lund, H., Bartling, S., Polley, C., Riaz, A., Senz, V., et al., 2021. Heat accumulation during femtosecond laser treatment at high repetition rate – a morphological, chemical and crystallographic characterization of self-organized structures on Ti6Al4V. Appl. Surf. Sci. 570, 151115. https://doi.org/10.1016/j.apsusc.2021.151115.

Sedao, X., Lenci, M., Rudenko, A., Faure, N., Pascale-Hamri, A., Colombier, J.P., et al., 2019. Influence of pulse repetition rate on morphology and material removal rate of ultrafast laser ablated metallic surfaces. Opt Laser. Eng. 116, 68–74. https://doi.org/10.1016/j.optlaseng.2018.12.009.

Sedao, X., Abou Khalil, A., 2022. Fonctionnalisation de surface par laser ultrarapide - Applications et voies vers l'industrialisation. Traitements des métaux. https://doi.org/10.51257/a-v1-re297.

Toloei, A., Stoilov, V., Northwood, D., 2013. The relationship between surface roughness and corrosion. In: Advanced Manufacturing, 2B. American Society of Mechanical Engineers, San Diego, California, USA, V02BT02A054. https://doi.org/10.1115/IMECE2013-65498.

Tournier, R., 1982. Polissage mécanique. Traitements des métaux. https://doi.org/10.51257/a-v1-m1495.

Tuck, B., 1975. The chemical polishing of semiconductors. J. Mater. Sci. 10, 321–339. https://doi.org/10.1007/BF00540357.

Valette S. Effets thermiques dus à l'interaction laser-matière dans les métaux en régime femtoseconde n.d.

Von Der Linde, D., Sokolowski-Tinten, K., Bialkowski, J., 1997. Laser–solid interaction in the femtosecond time regime. Appl. Surf. Sci. 109–110, 1–10. https://doi.org/10.1016/S0169-4332(96)00611-3.

Žemaitis, A., Gaidys, M., Gečys, P., Barkauskas, M., Gedvilas, M., 2021. Femtosecond laser ablation by bibursts in the MHz and GHz pulse repetition rates. Opt Express 29, 7641. https://doi.org/10.1364/OE.417883.

Zhao, D., Lu, X., 2013. Chemical mechanical polishing: theory and experiment. Friction 1, 306–326. https://doi.org/10.1007/s40544-013-0035-x.